Process Intensification of Catalytic Hydrogenation of Ethylanthraquinone with Gas-Liquid Microdispersion

J. Tan, J. S. Zhang, Y. C. Lu, J. H. Xu, and G. S. Luo
Dept. of Chemical Engineering, The State Key Lab of Chemical Engineering, Tsinghua University, Beijing 100084, China

DOI 10.1002/aic.12670
Published online June 8, 2011 in Wiley Online Library (wileyonlinelibrary.com).

In this article, to miniaturize the hydrogenation reactor and make the H_2O_2 production with more safety a gas-liquid microdispersion system was generated to intensify the process of catalytic hydrogenation of ethylanthraquinone by passing the gas-liquid microdispersion system through a generally packed bed reactor. A microdispersion device with a 5 μm pore size microfiltration membrane as the dispersion medium has been developed and microbubbles in the size of 10–100 μm were successfully generated. The reaction and mass transfer performance was evaluated. The conversion of ethylanthraquinone as much as 35% was realized in less than 3.5 s. The overall volume mass transfer coefficient in the microdispersion reaction system reached in the range of 1–21 s^{-1}, more than two orders of magnitude larger than the values in normal gas-liquid trickle-bed reactors. A mathematical model in the form of $Sh = 2.0 + 54.7Sc^{1/3}We^{1/2}\Phi^{1/10}$ has been firstly suggested, which can well predict the overall mass transfer coefficient. © 2011 American Institute of Chemical Engineers *AIChE J,* 58: 1326–1335, 2012

Keywords: gas-liquid, hydrogenation, microdispersion, mass transfer

Introduction

Hydrogen peroxide (H_2O_2) is a popular oxidizing agent, not only for its efficient oxidizing,[1,2] but also for its significant environmental friendliness as the by-product of oxidation reactions is water.[3,4] In commercial, Reidl-Pfleiderer process, which has a significant advantage of avoiding direct contact of H_2 and O_2, is widely used to produce hydrogen peroxide. Reactions involved in this process have been described by Drelinkiewicz et al.[5] and Halder and Lawal[6] The main reaction is shown as Figure 1a, in which 2-ethyl-9,10-anthraquinone (EAQ) is used as 'hydrogen carrier'. In this process, EAQ dissolved in an organic solvent is first hydrogenated to 2-ethylanthrahydroquinone ($EAQH_2$), with Pd or Ni as catalyst. H_2O_2 is then produced by the oxidation of $EAQH_2$ with O_2 in air. In addition to participating in the main reaction, $EAQH_2$ can also be converted to tetrahydro-2-ethylanthrahydroquinone (H_4EAQH_2) by further hydrogenation. As shown in Figure 1b, H_4EAQ can also be used as 'hydrogen carrier', forming H_4EAQ cycle route of H_2O_2 production. $EAQH_2$ may also take part in some side reactions, as shown in Figure 1c.

In the Reidl-Pfleiderer process, catalytic hydrogenation of EAQ is the key reaction in the synthesis of H_2O_2, in which efficient gas-liquid mixing and high mass transfer performance are demanded. As reported by Santacesaria et al.,[8] catalytic hydrogenation of antraquinone is a fast reaction and the reaction rate is controlled by the mass transfer resistance in conventional reactors. The enhancement of mass transfer can lead to higher reaction rate in catalytic hydrogenation of

Correspondence concerning this article should be addressed to G. S. Luo at gsluo@tsinghua.edu.cn.

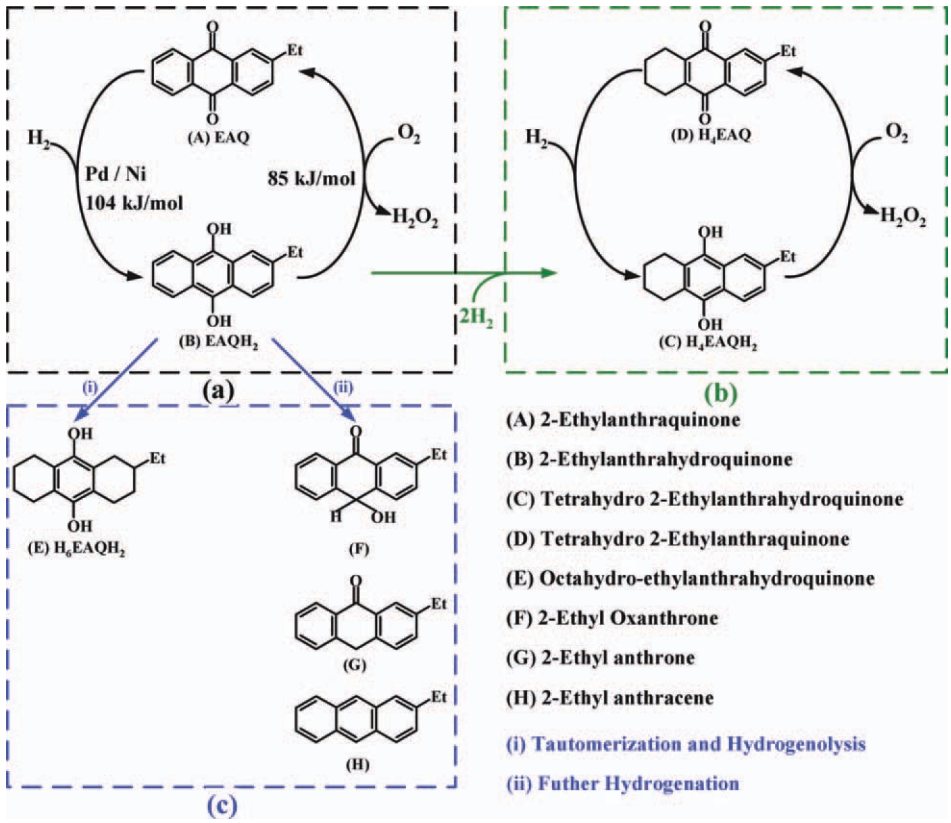

Figure 1. Reactions involved in the production of hydrogen peroxide.

(a) EAQ cycle route of H_2O_2 production; (b) H_4EAQ cycle route of H_2O_2 production; (c) Side reaction products. (The heat of reactions are given by Kirk-Othmer[7]) [Color figure can be viewed in the online issue, which is available at wileyonlinelibrary.com.]

EAQ and thus the reduction of reactor volume. Thus, the enhancement of mass transfer will possibly lead to a reaction process with higher safety, lower cost and higher environmental friendship, which is an expected direction.

Since the 21st century, microreactors have caught the attention of many researchers for its intensification of mixing and mass transfer rates[9,10] and have been used to realize multiphase reactions efficiently.[11–16] In particular, catalytic hydrogenation has been carried out in microchannel reactors[17] and micro-packed-bed reactors,[18,19] showing much higher reaction rate than in conventional reactors. Catalytic hydrogenation of EAQ in a microreactor has been studied by Halder and Lawal,[6] in which a T-junction microchannel was used to form a gas-in-liquid microdispersion system, and a following micro-packed-bed reactor was used to carry out the catalytic hydrogenation, showing much higher reactor space-time yield than in conventional reactors. The study[6] indicates that the bubble-in-liquid microdispersion system leads to the process intensification of catalytic hydrogenation, by enhancing the mass transfer process, showing that the reaction rate is controlled by mass transfer even in the microchannel reactor. However, the effect of dispersion state on mass transfer performance in packed-bed reactor or catalytic hydrogenation reaction of EAQ have not been investigated yet. As described in literature,[20] when a T-junction microchannel is used to form gas-liquid dispersion system to realize the physical absorption of CO_2 with water, the dispersion size, i.e. the equivalent diameter of bubble, ranges in 500–1500 μm and accordingly the overall mass transfer coefficient ranged from 4×10^{-4} to 1.6×10^{-3} m/s. The decrease in dispersion size will possibly lead to further intensification of the catalytic hydrogenation process, because mass transfer is the rate-controlling step. In our previous study, a microfiltration membrane has been used as at high throughput dispersion medium, to enhance the mass transfer performance in gas/liquid[21] and liquid/liquid[22] heterogeneous systems as well as the mixing process in liquid–liquid homogeneous systems.[23–25] In these studies, the dispersion size ranged in 10 to 20 times of the nominal pore size of the microfiltration membrane and the microdispersion systems did demonstrate very high mass transfer rate and good mixing efficiency.

In this study, for realizing the application of microdispersion reactions in large scale processes, a 5 μm pore size microfiltration membrane was used as the dispersion medium to form microbubble-in-liquid system. The gas-liquid microdispersion system flowed through a packed bed reactor, which was filled with Pd-Al_2O_3 particles inside, to realize catalytic hydrogenation of EAQ. The reaction and mass transfer performance was evaluated and the effects of flow rates, addition of inertial gas (N_2 as example), partial pressure of H_2, EAQ concentration and reaction temperature on them were studied. The mass transfer performance was compared with traditional equipment, and a new correlation was set up to predict the mass transfer performance, by considering the influence of diffusion coefficient, microdispersion

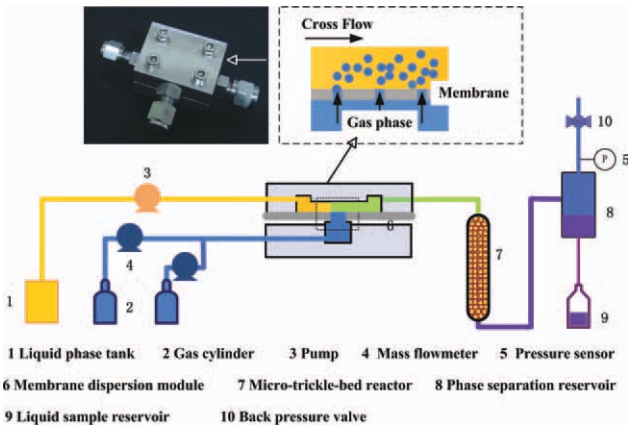

Figure 2. The equipment set-up.

[Color figure can be viewed in the online issue, which is available at wileyonlinelibrary.com.]

process and gas volume fraction, which potentially helps the design of the new process.

Experimental

Experimental set-up

The experimental set-up is shown in Figure 2. The membrane dispersion module was fabricated by stainless steel. A stainless steel microfiltration membrane (Figure 3) with 5 μm average pore size and 0.3 mm thickness was used as the dispersion medium. The active membrane area was 10 mm^2. The size of the flow channel was 15 mm $\times$ 2 mm $\times$ 3 mm. The size of the gas buffer reservoir was 10 mm $\times$ 5 mm $\times$ 10 mm. The liquid phase was pumped into the top side of the membrane (the flow channel) while the gas phase was pumped into the gas chamber. Under the action of pressure difference, the gas phase was dispersed as microsize bubbles when it passed through the membrane into the liquid phase to form a microdispersion system.

The formed microdispersion system flowed out of the membrane dispersion module and into a tubular reactor packed with Al_2O_3-supported-palladium-catalyst. The reactor was made of stainless steel tube with an inner diameter of 10 mm and a length of 50cm filled with catalyst particles. The size of the catalyst particles was around 3 mm and the bulk density was in the range of (0.63 $\pm$ 0.05) g/mL. In this study, 20.44 g of supported catalyst containing 0.3% $\pm$ 0.02% (w/w) palladium were used.

The reactor was connected to a phase separator with an inner diameter of 10 mm and height of 30 cm. The gas-liquid system flowed into the phase separator from the middle position and was separated into gas-phase and liquid-phase almost immediately for the larger density difference of the two phases. The separated gas-phase and liquid-phase flowed out of the separator from the top and bottom respectively.

An advection pump [(0–100) mL/min, with a measurement accuracy of $\pm$1%] was used to pump the liquid phase into the microcontactor. Two mass flowmeters (0-500 SCCM, with a measurement accuracy of $\pm$1.5%) were used to control feeding gases with stable pressure and flow rates.Three water baths (room temperature $-$100°C, with a resolution of $\pm$0.1°C) were used to maintain all the temperature of feed pipes, membrane dispersion module, packed bed reactor and phase separator to the required temperature.

A back pressure valve [(0 to 1.0) MPa range] was used to control the outlet pressure of the phase separator to the required pressure. A pressure sensor (0–0.5 MPa, with the accuracy of $\pm$0.5%) was installed before the back pressure valve to determine the total pressure of the gas phase.

Materials

Only fresh EAQ solution was used as solute in all the experiment, to avoid the effect of the degradation products. The solvent of EAQ solution was a mixture of 1,2,4-trimethylbenzene and trioctyl phosphate with the weight ratio of 1:2.6. EAQ, 1,2,4-trimethylbenzene and trioctyl phosphate were all reagent grade and purchased from Beijing Chemical Plant.

Hydrogen (H_2) and nitrogen (N_2) were taken as the gas components. H_2 and N_2 used in the experiment were all with purity of 99.995 mol % were purchased from Beijing Huayuan Gas Chemical Industry.

The catalyst used in this study was 0.3% $\pm$ 0.02% (w/w) Pd supported on Al_2O_3 and was provided by Sinopec Group.

Apparatus and analysis

The microbubble size was measured using a high-speed CCD video camera which was connected to the microscope with magnification of 40.

The liquid product was analyzed with the same method as described in literature.[6] The liquid product was oxidized completely by O_2 until the color of the solution completely changed, extracted twice with 1% (w/w) phosphoric acid and titrated with standard potassium permanganate solution with the concentration of 0.026 mol/L, to determine the concentration of total hydrogenated anthraquinones. The accuracy of titration is 0.02 mL of standard potassium permanganate solution.

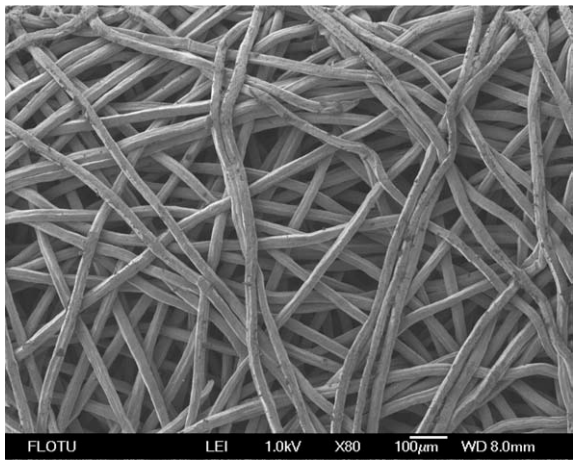

Figure 3. The SEM picture of the microfiltration membrane surface.

Results and Discussion

Effect of flow rates on conversion

In this study, the conversion of EAQ is calculated as Eq. 1

$$\text{Conversion} = \frac{C_{\text{EAQH}_2}}{C_{\text{EAQ},0}} \tag{1}$$

where,

C_{EAQH_2} is the concentration of EAQH_2 after reaction, which is determined by assuming EAQH_2 to be the only product of hydrogenation, mol/L;

$C_{\text{EAQ},0}$ is the initial concentration of EAQ, mol/L.

As reported in the literature,[6,8] catalytic hydrogenation of antraquinone is a fast reaction and the reaction rate is controlled by the mass transfer process. Thus the control step of this reaction process is assumed to be mass transfer here. The overall volume mass transfer coefficient, $K_L a$, is calculated by Eq. 2

$$K_L a = \frac{R}{\overline{C^*_{\text{H}_2}}} \tag{2}$$

where

$K_L a$ is the overall volume mass transfer coefficient, s^{-1};

R is the overall reaction rate in the liquid phase, mol/(m^3 s);

$\overline{C^*_{\text{H}_2}}$ is the average saturated solubility of H_2 in the solvent, mol/m^3, which is calculated by

$$\overline{C^*_{\text{H}_2}} = \frac{(C^*_{\text{H}_2,1} - C^*_{\text{H}_2,2})}{\ln(C^*_{\text{H}_2,1}/C^*_{\text{H}_2,2})} \tag{3}$$

where

$C^*_{\text{H}_2,1}$ is the solubility of H_2 before reaction, mol/m^3;

$C^*_{\text{H}_2,2}$ is the solubility of H_2 after reaction, mol/m^3.

Considering the similarity of H_2 solubility in organic solvent, the solubility of H_2 in organic solution in this study is considered to be the same value as H_2 in working solution in which the mixture of n-hexane and xylene is used as solvent, as described as following[26]

$$C^*_{\text{H}_2}/(\text{mol/m}^3) = (-3.407 + 0.019(T/\text{K}))(p_{\text{H}_2}/0.987\ \text{atm}) \tag{4}$$

where

p_{H_2} is the partial pressure of H_2 in the gas phase.

The effect of the H_2 volume flow rate, Q (H_2), for a certain phase ratio at different molar ratio of H_2 to EAQ, on the conversion of EAQ, is shown in Figures 4–6a, when the reaction temperature of 30, 50, and 60°C, respectively. In all the temperature and molar ratio, the conversion increases with the increase of the flow rate at first, possibly due to the increase in specific interfacial area. As shown in Figure 7, the bubble size and dispersity both decrease with increasing liquid phase flow rate at a constant gas phase flow rate. As the flow rate increases further, the conversion begins to decrease due to the reduction in residence time.

The overall volume mass transfer coefficient according to the situation of Figures 4–6a is shown in Figures 4–6b. $K_L a$ increases with the increase in the flow rate of liquid phase,

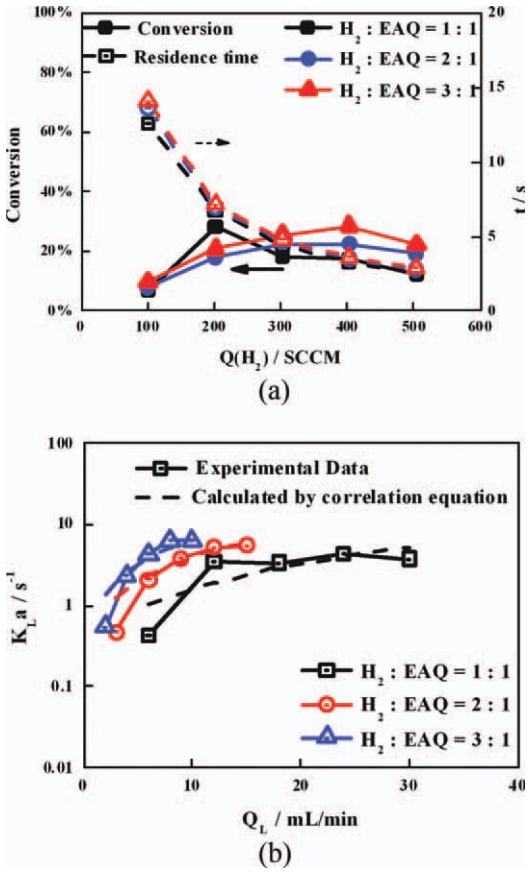

Figure 4. (a) Effect of H_2 volume flow rate, for a constant phase ratio at different molar ratio of H_2 to EAQ, on the conversion of EAQ; (b) Effect of liquid flow rate on overall volume mass transfer coefficient.

(Temperature: 30°C, EAQ concentration: $C_{\text{EAQ}} = 0.6$ mol/L, H_2 partial pressure at inlet: $P(H_2) = 320$kPa, N_2 volume fraction at inlet: $\varphi(N_2) = 20\%$, the experimental uncertainty of the conversion of EAQ and overall volume mass transfer coefficient are respectively less than 0.46% and 0.05 s^{-1}, in which the error of titration is mainly considered) [Color figure can be viewed in the online issue, which is available at wileyonlinelibrary.com.]

Q_L, at a constant phase ratio. As shown in our previous study,[27] the dispersion size is proportional to $Q_L^{-0.20}$. As the increase in the flow rate of liquid phase, the dispersion size decreases, which leads to higher mass-transfer area as well as thinner liquid film around bubbles. The decrease in the thickness of liquid film causes the decrease in mass-transfer residence. Both the increase in mass-transfer area and the decrease in mass-transfer residence, cause the increase in $K_L a$ together. The model which describes the experimental results is developed further and it will be discussed later.

Effect of addition of N_2 on conversion

As described in the literature,[28] the addition of inert component (N_2 as a best choice) will increase the stability of the pressure drop in the trickle bed as well as the selectivity of the catalyst. Thus, N_2 is added in the gas feed in this study and the effect of the volume fraction of N_2 in the feed of

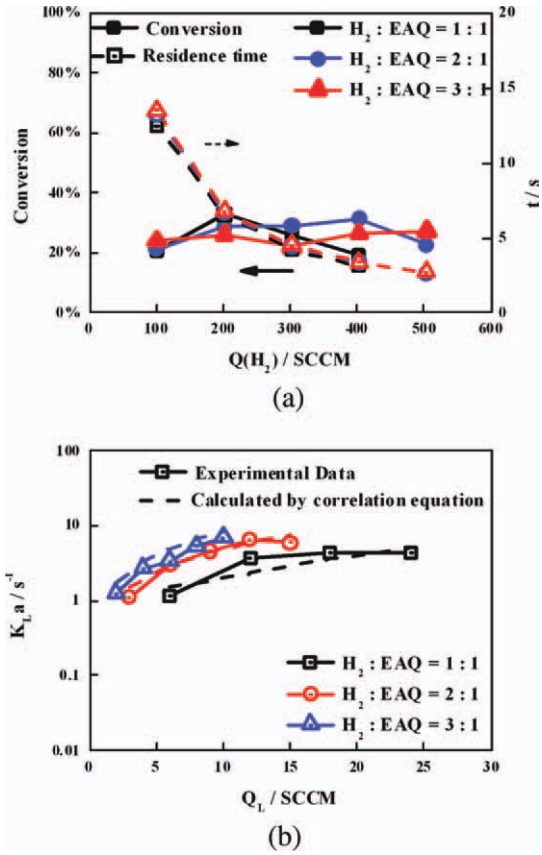

Figure 5. (a) Effect of H_2 volume flow rate, for a constant phase ratio at different molar ratio of H_2 to EAQ, on the conversion of EAQ; (b) Effect of liquid flow rate on overall volume mass transfer coefficient.

(Temperature: 50°C, EAQ concentration: C_{EAQ} = 0.6 mol/L, H_2 partial pressure at inlet: $P(H_2)$ = 320kPa, N_2 volume fraction at inlet: $\varphi(N_2)$ = 20%) [Color figure can be viewed in the online issue, which is available at wileyonlinelibrary.com.]

gas phase is investigated here. As shown in Figure 8a, when keeping a constant H_2 partial pressure (the total pressure at the outlet is adjusted to keep a constant H_2 partial pressure) and molar ratio of H_2 to EAQ, the addition of N_2 does not show significant influence on the conversion. It is worth noting that the conversion of EAQ reaches about 35% in less than 3.5 s when the liquid flow rate is 12 mL/min, while the time required to reach the same conversion in conventional reactor is about 1.27 min, as reported in literature.[28] The overall volume mass transfer coefficient accordingly is shown in Figure 8b, indicating that the addition of N_2 does not show influence on K_La.

Effect of partial pressure of H_2 on conversion

The effect of the partial pressure of H_2 in the feed of gas phase on the conversion of EAQ is shown in Figure 9a. The conversion of EAQ increases slightly with the increase in the partial pressure of H_2. The overall volume mass transfer coefficient accordingly is shown in Figure 9b, indicating that K_La decreases as the increase in H_2 partial pressure. As the increase in H_2 partial pressure, the gas-to-liquid flow rate ratio decreases, and the thickness of the liquid film around the bubble increases, leading to the increase in the mass-transfer residence and the decrease in K_La. The model which describes the experimental results is developed further and it will be discussed later.

Effect of EAQ concentration on conversion

The effect of EAQ concentration on the conversion of EAQ and the concentration of H_2O_2 in the product, at a constant molar ratio of H_2 to EAQ, are shown in Figures 10a, b, respectively. The conversion of EAQ decreases significantly while the concentration of H_2O_2 in the product increases slightly as the increase in EAQ concentration.

The overall volume mass transfer coefficient accordingly is shown in Figure 10c, indicating that K_La increases as the increase in EAQ concentration. As the increase in EAQ concentration, the gas-to-liquid flow rate ratio, and the thickness of the liquid film around the bubble increases, leading to the decrease in the mass-transfer residence and the increase in K_La. The model which describes the experimental results is developed further and it will be discussed later.

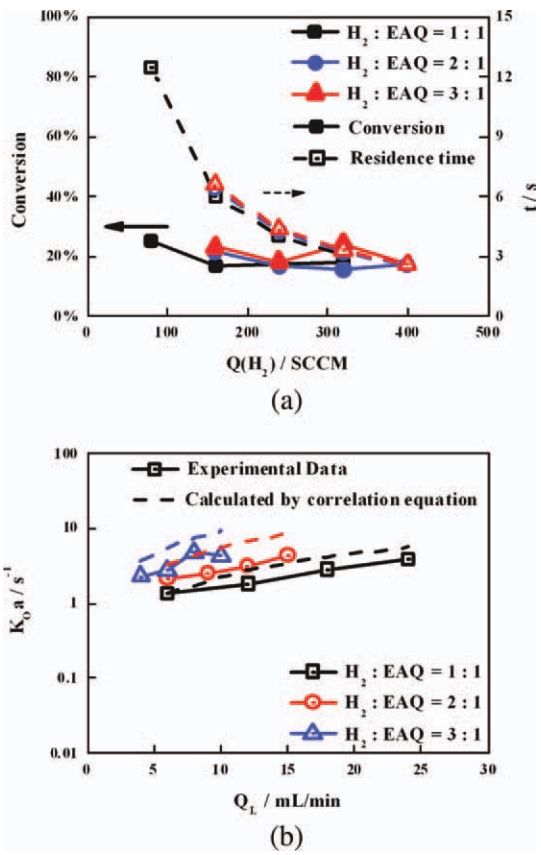

Figure 6. (a) Effect of H_2 volume flow rate, for a constant phase ratio at different molar ratio of H_2 to EAQ, on the conversion of EAQ; (b) Effect of liquid flow rate on overall volume mass transfer coefficient.

(Temperature: 60°C, EAQ concentration: C_{EAQ} = 0.6 mol/L, H_2 partial pressure at inlet: $P(H_2)$ = 320kPa, N_2 volume fraction at inlet: $\varphi(N_2)$ = 20%) [Color figure can be viewed in the online issue, which is available at wileyonlinelibrary.com.]

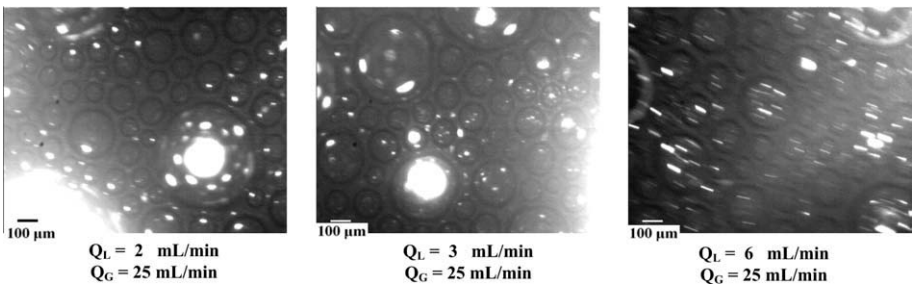

Figure 7. Microbubble photos at different operation conditions.

Effect of reaction temperature on conversion

The effect of reaction temperature on the conversion of EAQ is shown in Figure 11a, indicating that the conversion of EAQ increases with the increase in the temperature significantly. The overall volume mass transfer coefficient accordingly is shown in Figure 11b, indicating that K_La increases slightly with the increase in temperature. As the increase in temperature, the diffusion coefficient of H_2 in working solution increases, leading to the increase of K_La.

Correlation of K_La

In "Effect of flow rates on conversion" to "Effect of reaction temperature on conversion" sections, the effect of flow rates, the addition of N_2, H_2 partial pressure, EAQ concentration and reaction temperature on EAQ conversion as well as the overall volume mass transfer coefficient are presented. The results show that K_La in this microdispersion process ranges in

$$K_La \approx 1 - 21\ s^{-1}$$

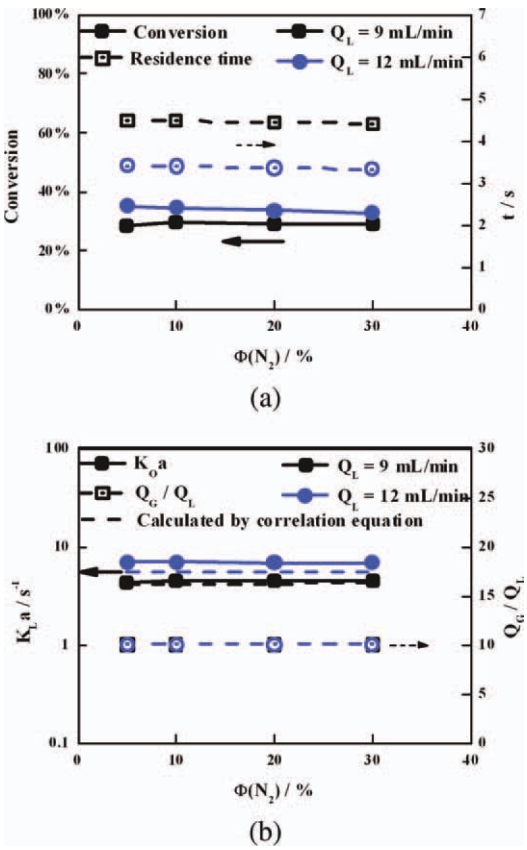

Figure 8. Effect of the volume fraction of N_2 in the feed of gas phase on (a) conversion of EAQ; (b) the overall volume mass transfer coefficient.

(Temperature: 50°C, C_{EAQ} = 0.6 mol/L, $P(H_2)$ = 320kPa, Molar ratio of H_2 and EAQ at inlet: H_2: EAQ = 2:1) [Color figure can be viewed in the online issue, which is available at wileyonlinelibrary.com.]

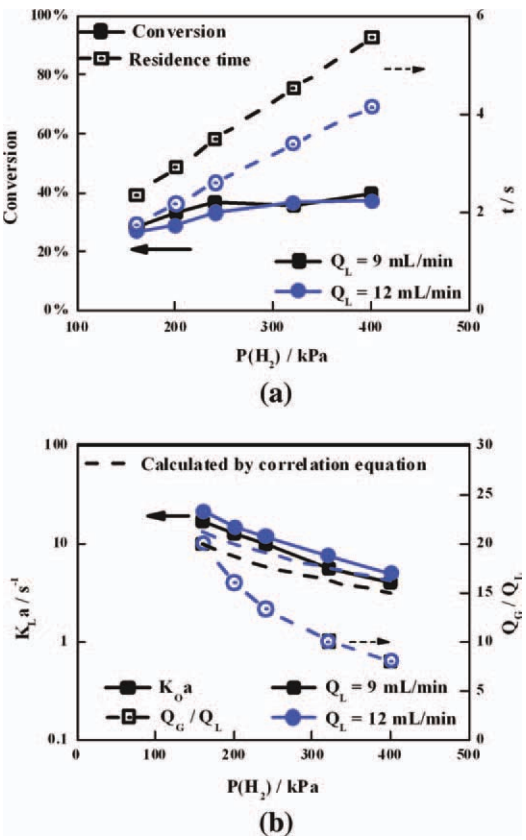

Figure 9. Effect of the H_2 partial pressure in the feed of gas phase on (a) the conversion of EAQ; (b) the overall volume mass transfer coefficient.

(Temperature: 50°C, C_{EAQ} = 0.6 mol/L, $\varphi(N_2)$ = 20%, H_2:EAQ = 2:1) [Color figure can be viewed in the online issue, which is available at wileyonlinelibrary.com.]

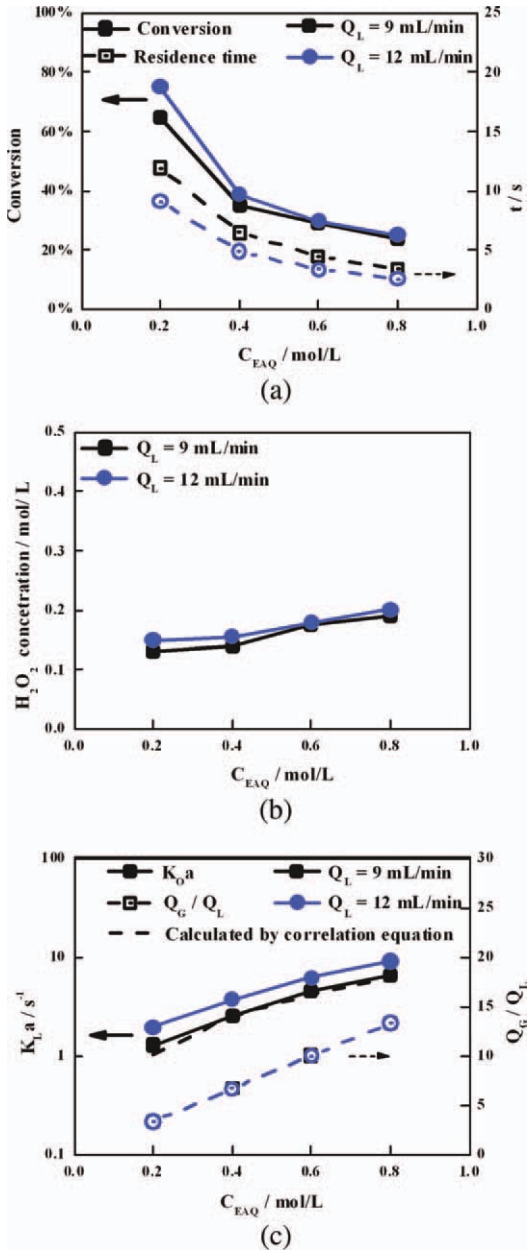

Figure 10. Effect of the EAQ concentration on the (a) EAQ conversion; (b) H_2O_2 concentration in the product; (c) the overall volume mass transfer coefficient.

(Temperature: 50°C, $P(H_2)$ = 320 kPa, $\varphi(N_2)$ = 20%, H_2:EAQ = 2:1) [Color figure can be viewed in the online issue, which is available at wileyonlinelibrary.com.]

Such values are more than two orders of magnitude larger than the values for laboratory trickle-bed[29]

$$K_L a \approx 0.01 - 0.08\ s^{-1}$$

The great improvement of $K_L a$ is possibly due to the large interfacial area and short mass transfer distance caused by the microsized dispersion and leads to the good performance in catalytic reaction process.

The correlation of $K_L a$ will help for the prediction the process in catalyzed gas-liquid reactions controlled by mass transfer and thus the design of the reactors for this kind of reaction. In the literature, some correlations have been developed to predict the mass transfer performance from the liquid to the surface of solid, in most of which viscosity force and inertial force are considered to be the main factors affecting the mass transfer process and dimensionless numbers of Sc and Re_p are usually used to predict Sh. The dimensionless numbers of Sc, Re_p, and Sh are defined as Eqs. 5–8

$$\mathrm{Sc} = v/D \tag{5}$$

where

v is the kinematic viscosity of the liquid, m^2/s;

D is the diffusion coefficient of the component in liquid, m^2/s. Considering the similarity of the diffusion coefficient of H_2 in organic solvent, the diffusion coefficient of H_2 in organic solution in this study is considered to be the same value as H_2 in working solution in which the mixture of n-hexane and xylene is used as solvent, as described as following[26]

$$D_{H_2}/(\mathrm{m/s^2}) = 1.27 \times 10^{-6} \exp(-1520/T) \tag{6}$$

where

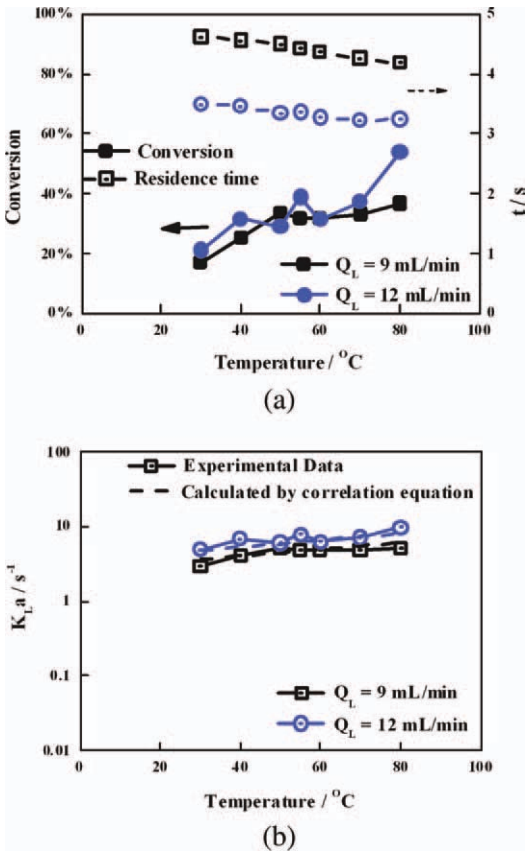

Figure 11. Effect of reaction temperature on (a) the conversion of EAQ; (b) the overall volume mass transfer coefficient.

(C_{EAQ} = 0.6 mol/L, $P(H_2)$ = 320 kPa, $\varphi(N_2)$ = 20%, H_2:EAQ = 2:1) [Color figure can be viewed in the online issue, which is available at wileyonlinelibrary.com.]

T is the temperature, K

$$Re_P = du/v \tag{7}$$

where

d is the diameter of the solid, m;

u is the superficial velocity of the liquid flowing on the surface of the solid, m/s

$$\mathrm{Sh} = k_L d/D \tag{8}$$

The correlation of Sh, Sc, and Re_p is

$$\mathrm{Sh} = 2.0 + 1.1\ \mathrm{Sc}^{1/3}\ Re_P^{1/2} \tag{9}$$

as reported in the literature[30] and

$$\mathrm{Sh} = 2.0 + 1.8\ \mathrm{Sc}^{1/3} Re_P^{3/5} \tag{10}$$

as in literature.[31] However, the two correlations above can not be used in this microdispersion system, for Sh calculated by experimental data is almost more than 5 times higher than the predicted value, as shown in Figure 12.

The significant deviation indicates that the correlations are not suitable for the microdispersion system, which is possibly caused by the different flow patterns between liquid-flow-through-solid-surface and foam-flow-through-solid-surface. In the traditional device, the gas phase and liquid phase concurrently flow through the packed bed, thus the mass transfer process from gas phase to solid surface is controlled by the mass transfer of gas dissolved in the liquid from gas-liquid interface to liquid-solid interface. The main factors affecting this mass-transfer process are: the diffusion coefficient of gas in liquid (affecting on the rate of diffusion mass transfer) and the flow condition of the liquid (affecting on the convective mass transfer). Thus, Re_p and Sc are used in the correlation to predict the mass-transfer coefficient in liquid-flow-through-solid-surface flow pattern. When the gas phase is dispersed as microbubbles into the liquid phase before passing through packed bed, the new flow pattern of foam-flow-through-solid-surface is formed. The flow condition and thickness of the liquid film on particle surface will be different from the traditional process. The microbubble-in-liquid system with the new flow pattern could be considered to be a uniform fluid, which passes through the solid surface and forms fluid/solid system. As is well known that the diffusivity in the liquid phase is much lower than in the gas phase, thus, the controlling step of external mass-transfer is mass transfer of the gas dissolved in the liquid through the liquid film to the solid surface. In this case, Sh number could be calculated with K_L and the diffusivity D. D could be considered as the gas diffusivity in the liquid phase, which can be determined by Eq. 6. For the new flow pattern, mass transfer will be affected by new factors and new correlation needs to be developed. As shown in Figures 4–6b, K_La increases with the increase in the flow rate of liquid phase, Q_L, at a constant phase ratio, which is possibly due to the decrease in the liquid film thickness on the particle surface. On the other hand, as shown in our previous study,[27] the microbubble size is proportional to $Q_L^{-0.20}$, thus the increase of K_La is possibly due to the decrease in the dispersion size and thus the

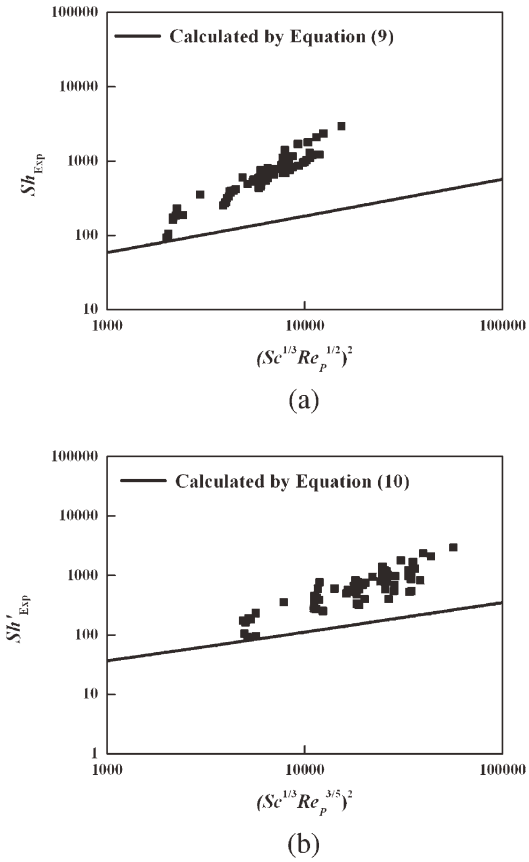

Figure 12. The comparison of Sh calculated from experimental values and correlation Eqs. 9 and 10.

increase in gas-liquid interfacial area. As shown in Figures 7–9b, K_La does not change at constant flow rates and decreases with the increase in the gas-to-liquid phase ratio at a constant liquid flow rate, Q_L. The effect of phase ratio on K_La is possibly due to the decrease in the thickness of the liquid film as the increase in the phase ratio. As shown in Figure 10b, K_La increases slightly with the increase in temperature, possibly due to the decrease in the liquid film thickness too. As described above, the main factors affecting the mass transfer performance of foam-flow-through-solid-surface are: the foam flow condition and the thickness of the liquid film. The liquid film is determined by two factors: the size of the dispersed bubbles and the gas-to-liquid flow rate ratio. As described above, there are new factors effecting the mass-transfer process in the flow pattern of foam-flow-through-solid-surface: inertial force, which affecting on the dispersion size, and gas-to-liquid flow rate ratio, which affecting on the thickness of the liquid film around bubbles. Thus We and Φ are introduced into the new empirical equation, instead of Re_p, in which We and Φ are defined as Eqs. 11 and 12

$$\mathrm{We} = \rho u^2 d/\gamma \tag{11}$$

where

γ is the interfacial tension of gas and liquid, N/m

$$\Phi = Q_G/(Q_G + Q_L) \tag{12}$$

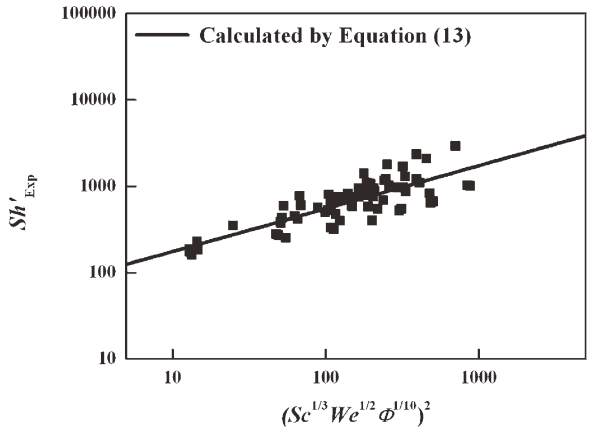

Figure 13. The comparison of Sh calculated from experimental values and the correlation equation.

where

Q_G is the flow rate of the gas phase, mL/min;

Q_L is the flow rate of the liquid phase, mL/min.

The correlation equation is determined as

$$\mathrm{Sh} = 2.0 + 54.7\ \mathrm{Sc}^{1/3}\mathrm{We}^{1/2}\Phi^{1/10} \tag{13}$$

As shown in Figure 13, the correlation as Eq. 13 shows good coincidence with experimental values.

Conclusion

In this article, a gas-liquid microdispersion device with a 5 μm pore size microfiltration membrane as the dispersion medium has been developed to generate gas-liquid microdispersion systems for process intensification of catalytic hydrogenation of ethylanthraquinone. Using the device microbubbles in the size of 10–100 μm were successfully generated with ethylanthraquinone solution as the continuous phase. The reaction and mass transfer performance was evaluated and the effects of flow rates, addition of inertial gas (N_2 as example), partial pressure of H_2, EAQ concentration and reaction temperature on them were studied. By passing the gas-liquid microdispersion system through a packed bed reactor the conversion of ethylanthraquinone as much as 35% was reached in less than 3.5 s. The overall volume mass transfer coefficient in the microdisperion system was calculated and the value ranged in 1–21 s^{-1}, which is more than two orders of magnitude larger than the values in the normal gas-liquid trickle-bed reaction processes. The results indicate that gas-liquid microdispersion can make great improvement to solid catalyzed gas-liquid reactions which are controlled by mass transfer. An equation has been developed to correlate the mass transfer in the flow pattern of foam-flow-through-solid-surface with diffusion coefficient, inertial force, thickness of the liquid film and bubble size, which shows good coincidence with experimental values. The research may provide an effective way to miniaturize the hydrogenation reactor and make the H_2O_2 production with more safety.

Acknowledgments

The authors acknowledge the support of the National Natural Science Foundation of China (20876084, 21036002) and National Basic Research Program of China (2007CB714302) for this work.

Literature Cited

1. Strukul G. *Catalytic Oxidations with Hydrogen Peroxide as Oxidant*. In: Strukul G, editor. Dordrecht: Kluwer, 1992:1–11.
2. Goor G. *Catalytic Oxidations with Hydrogen Peroxide as Oxidant*. In: Strukul G, editor. Dordrecht: Kluwer, 1992:13–43.
3. Tundo P, Anastas P, Black DS, Breen J, Collins T, Memoli S, Miyamoto J, Polyakoff M, Tumas W. Synthetic pathways and processes in green chemistry. Introductory overview. *Pure Appl Chem*. 2000;72:1207–1228.
4. Anastas PT, Warner JC. *Green Chemistry: Theory and Practice*. NewYork: Oxford University Press, 1998.
5. Drelinkiewicz A, Laitinen R, Kangas R, Pursiainen J. 2-Ethylanthraquinone hydrogenation on Pd/Al_2O_3: the effect of water and NaOH on the degradation process. *Appl A Catal A: Gen*. 2005;284:59–67.
6. Halder R, Lawal A. Experimental studies on hydrogenation of anthraquinone derivative in a microreactor. *Catal Today*. 2007;125:48–55.
7. Kirk RE, Othmer DF. *Encyclopedia of Chemical Technology*. New York: Wiley, 971.
8. Santacesaria E, Di Serio M, Russo A, Leone U, Velotte R. Kinetic and catalytic aspects in the hydrogen peroxide production via anthraquinone. *Chem Eng Sci*. 1999;54:2799–2806.
9. Jorgensen K, Jensen AD, Sloth J, Dam-Johansen K, Bach P. Comments to "Analysis of constant rate period of spray drying of slurry." *Chem Eng Sci*. 2007;62:2096–2108.
10. Yue J, Luo LG, Gonthier Y, Chen GW, Yuan Q. An experimental investigation of gas–liquid two-phase flow in single microchannel contactors. *Chem Eng Sci*. 2008;63:4189–4202.
11. Tegrotenhuis WE, Cameron RJ, Viswanathan VV, Wegeng RS. Solvent extraction and gas absorption using microchannel contactors. Presented at the 3rd International Conference on Microreaction Technology, New Orleans, LA, April 18–21 1999:541–549.
12. Chambers RD, Holling D, Spink RCH, Sandford G. Gas–liquid thin film microreactors for selective direct fluorination. *Lab Chip*. 2001;1:132–137.
13. Hessel V, Ehrfeld W, Golbig K, Haverkamp V, LDw H, Stor M, Wille C, Guber A, Jnhnisch K, Baerns M. Gas/liquid microreactors for direct fluorination of aromatic compounds using elemental fluorine. Presented at the 3rd International Conference on Microreaction Technology, New Orleans, LA, April 18–21 1999:526–540.
14. Jahnisch K, Baerns M, Hessel V, Ehrfeld W, Haverkamp W, LDwe H, Wille C, Guber A. Direct fluorination of toluene using elemental fluorine in gas/liquid microreactors. *J Fluorine Chem*. 2000;105:117–128.
15. Mas de N, Jackman RJ, Schmidt MA, Jensen KF. Microchemical systems for direct fluorination of aromatics. Presented at the 5th International Conference on Microreaction Technology, Strasbourg, France, May 27–30 2001:60–67.
16. Antes J, Tuercke T, Marioth E, Lechner F, Scholz M, SchnRrer F, Krause HH, LDbbecke S. Investigation, analysis and optimization of exothermic nitrations in microreactor processes. Presented at the 5th International Conference on Microreaction Technology, Strasbourg, France, May 27–30 2001:446–454.
17. Tadepalli S, Qian DY, Lawal A. Comparison of performance of microreactor and semi-batch reactor for catalytic hydrogenation of o-nitroanisole. *Catal Today*. 2007;125:64–73.
18. McGovern S, Harish G, Pai CS, Mansfield W, Taylor JA, Pau S, Besser RS. Multiphase flow regimes for hydrogenation in a catalyst-trap microreactor. *Chem Eng J*. 2008;135:S229–S236.
19. Trachsel F, Hutter C, von Rohr PR. Transparent silicon/glass microreactor for high-pressure and high-temperature reactions. *Chem Eng J*. 2008;135:S309–S316.
20. Yue J, Chen GW, Yuan Q, Luo LA, Gonthier Y. Hydrodynamics and mass transfer characteristics in gas–liquid flow through a rectangular microchannel. *Chem Eng Sci*. 2007;62:2096–2108.
21. Tan J, Xu JH, Wang K, Luo GS. Rapid measurement of gas solubility in liquids using a membrane dispersion micro-contactor. *Ind Eng Chem Res*. 2010;49:10040–10045.

22. Xu JH, Luo GS, Chen GG, Tan B. Mass transfer performance and two-phase flow characteristic in membrane dispersion mini-extractor. *J Membrane Sci*. 2005;249:75–81.
23. Chen GG, Luo GS, Xu JH, Wang JD. Membrane dispersion precipitation method to prepare nanopartials. *Powder Technol*. 2004;139:180–185.
24. Chen GG, Luo GS, Yang LM, Xu JH, Sun Y, Wang JD. Synthesis and size control of $CaHPO_4$ particles in a two-liquid phase micromixing process. *J Cryst Growth*. 2005;279:501–507.
25. Chen GG, Luo GS, Sun Y, Xu JH, Wang JD. A ceramic microfiltration tube membrane dispersion extractor. *AIChE J*. 2004;50:382–387.
26. Berglint T, Schoon NH. Kinetic and mass-transfer aspects of the hydrogenation stage of the anthraouinone process for hydrogen-peroxide production. *Ind Eng Chem Process Des Dev*. 1981;20:615–621.
27. Tan J, Du L, Xu JH, Wang K, Luo GS. Surfactant free microdispersion process of gas in organic solvents in microfluidic devices. *AIChE J*. In press.
28. Solvay SA. Making hydrogen peroxide by the anthraquinone process. Patent: GB 2334028A, 1998.
29. AlDahhan MH, Larachi F, Dudukovic MP, Laurent A. High-pressure trickle-bed reactors: a review. *Ind Eng Chem Res*. 1997;36:3292–3314.
30. Ranz WE. Friction and transfer coefficients for single particles and packed beds. *Chem Eng Progr*. 1952;48:247–253.
31. Wakao N, Funazkri T. Effect of fluid dispersion coefficients on particle-to-fluid mass-transfer coefficients in packed-beds-correlation of Sherwood number. *Chem Eng Sci*. 1978;33:1375–1384.

Manuscript received Jan. 8, 2011, and revision received Apr. 18, 2011.